Pergamon

International Journal of Machine Tools & Manufacture 42 (2002) 1145–1152

INTERNATIONAL JOURNAL OF
MACHINE TOOLS & MANUFACTURE
DESIGN, RESEARCH AND APPLICATION

The mechanisms of bell mouth formation in gundrilling when the drill rotates and the workpiece is stationary. Part 2: the second stage of drill entrance

V.P. Astakhov *

Hyper Tool Engr., 3319 Fulham Dr Rochester Hills, MI 48309, USA

Received 28 September 2001; received in revised form 17 April 2002; accepted 22 April 2002

Abstract

This paper reveals the main design and technological factors affecting entrance stability and provides practical recommendations on the design of gundrills. The subject has been covered in two parts. In the first part of this paper, the first stage of drill entrance, which begins when the gundrill touches the face of the workpiece and ends when the gundrill's cutting edges are fully engaged in cutting, is considered. The role of the clearance in the starting bush and the design of the gundrill's supporting area are analyzed. In this paper, the second stage of gundrill entrance is analyzed. The system engineering approach, which includes the time axis, is used in the consideration of distinctive steps in the drill entrance. The influence of the design parameter of the gundrill (such as relative location of the supporting area and the cutting edges, flank (relief) angle of the outer cutting edge, the location of the rake face, design and location of the supporting area) as well as the clearance in the starting bush on the duration of entrance instability is discussed. A number of practical suggestions to increase the entrance stability are provided.

Keywords: Gundrilling; Entrance stability; Supporting area; Supporting pads; Starting bush; Drill locating

1. Introduction

Cutting tool reliability in one of the most important economic considerations in automotive industry where an unscheduled stoppage of manufacturing lanes leads to significant loss of production time. To reduce these losses, the so-called unpredictable tool failures should be analyzed and thus reduced.

Among many tools used in automotive industry, gundrills eventually become responsible for a significant loss of production time. In our opinion it happens because not many research and development results and data are available on gundrilling compared to other tool types. The only book available on gundrilling is a small book published by the American Society of Tool and Manufacturing Engineers in 1967 [1]. Although this book remains a valuable source on drilling practice and many practical advises given in this book are still actual today, it describes what might be termed an 'evolutionary' stage of development. It fails to explain the different reasons why one or another drill design and component are being used, which one is better and when, what would happen if a particular parameter is altered, etc [2]. Moreover, the above mentioned book, having been written by practical engineers, does not provide any information on the most important geometrical parameters of drill point geometry, namely the rake and the relief (flank) angles, circular land and platform sizes, supporting area (pads) design, etc.

The gap in the knowledge on the influence of the gundrill design parameters on tool stability led to misunderstanding the concept of gundrill stability. For example, recent study [3] on the gundrill stability does not consider the essential design parameters of the tool and gundrilling system [2]. As a result, the mechanics of stability is missed and thus the stability model becomes insensitive to the essential parameters of the gundrilling system.

This paper is a continuation of the earlier Part 1 paper [4] in which the first stage of drill entrance is considered in details. This first stage extends from the moment the

* Tel.: +1-248-852-0246; fax: +1-248-852-0246.
E-mail address: astvik@mailcity.com (V.P. Astakhov).

0890-6955/02/$ - see front matter
PII: S0890-6955(02)00051-2

gundrill touches the face of the workpiece and ends when the outer and inner cutting edges are completely engaged in cutting. The objective of this paper is to consider the second stage of drill entrance.

2. The second stage of gundrill entrance as the entrance of the drill's cutting part and supporting elements

The second stage of gundrill entrance begins when the cutting edges are fully engaged with the workpiece. A logical question, which left unanswered in Part 1, is about the diameter of hole drilled at the first stage of drill entrance, which hereafter is referred to as the initial diameter d_{01}. This diameter depends on the position of the axis of rotation, i.e. what actually rotates in drilling. Among three possible methods of gundrilling, this paper considers the most common method when the gundrill rotates and the workpiece is stationary. This method is used when the workpiece is large or it has a non-symmetrical shape, which is not suitable for its rotation (a cylinder head, fuel pump housing, etc.). The use of this method imposes special requirements on the accuracy of the gundrill and gundrilling installation. The alignment of the gundrill components (that causes the so-called drill's whipping) should be next to perfect when drilling holes of relatively small diameter (less then 10 mm) in light materials such as aluminum alloys, i.e. when the rotational speed (6000–15,000 rpm) and the feed rate (600–1000 mm/min) are high. The clearance in the starting bush, drill holder-starting bush alignment, and the accuracy of the feed motion are the key factors in using this method.

2.1. The initial diameter

To calculate the initial diameter, we should refer to Fig. 1, which presents the case where the axis of drill rotation coincides with that of the starting bush. Moreover, it is assumed that the supporting pads and the periphery point P_R have the same radius R_{dr0}. When drill rotates and workpiece is stationary, the axis of rotation always coincides with that of the starting bush (center O in Fig. 1) and thus the initial diameter d_{01} calculates as

$$d_{01} = 2R_{dr1} \quad (1)$$

Using the same approach as in Sections 5.1 and 5.2 of Part 1, one can obtain the following equations for a gundrill having the supporting continuum

$$R_{dr1} = \sqrt{\Delta_{sb}^2 + R_{dr0}^2 - 2\Delta_{sb}R_{dr0}\cos\left(\frac{\pi}{2} - \varepsilon_1 + \mu_0\right)} \quad (2)$$

$$c_1 = c_0 + \Delta_{sb}\cos\varepsilon_1 \quad (3)$$

$$\mu_1 = \arcsin\frac{\Delta_{sb}\cos\varepsilon_1}{R_{dr1-W}} \quad (4)$$

where

$$\Delta_{sb} = \frac{1}{2}(d_{sb} - d_{dr}) \quad (5)$$

Here, d_{sb} and d_{dr} are the actual diameters of the starting bush and gundrill, respectively; ε_1 is the angle that the resultant force in the *xy*-plane makes with the *y*-axis (Part 1). The necessity and significance of c_0 and μ_0 have been discussed in Ref. [5].

For a gundrill having two supporting pads, these parameters calculate as

$$R_{dr1} = \sqrt{\Delta_{int}^2 + R_{dr0}^2 - 2\Delta_{int}R_{dr0}\cos\left(\frac{\pi}{2} - \varepsilon_1 + \mu_0\right)} \quad (6)$$

$$c_1 = c_0 + \Delta_{int}\cos\varepsilon_1 \quad (7)$$

$$\mu_1 = \arcsin\frac{\Delta_{int}\cos\varepsilon_1}{R_{dr1}} \quad (8)$$

It is understood that if $\Delta_{sb} = 0$, i.e. there is no clearance between the drill and the starting bush or this clearance is negligibly small, then

$$d_{01} = 2R_{dr0} \quad (9)$$

As discussed in Part 1, the cylindrical margin on the side cutting edge (represented by the periphery point P_R in the *xy*-plane) and the cylindrical surfaces of the supporting pads may not belong to the same cylinder (Fig. 1). If ρ_1 is the radial clearance between the cylinder containing the cylindrical surfaces of the supporting pads and that containing the cylindrical margin on the side cutting edge (the sign of ρ_1 is seen in Fig. 2) then Eqs. (1) and (9) become respectively

$$d_{01} = 2(R_{dr1-I} \pm \rho_1) \quad (10)$$

$$d_{01} = 2(R_{dr0} \pm \rho_1) \quad (11)$$

Experiments carried out for wide range of cutting regimes confirm these results.

2.2. System consideration of the second stage

The present study differs from any other known study in the fact that the time axis is considered according to the system engineering approach, as introduced in metal cutting studies by Astakhov [6,7]. According to this approach, the process of drill entrance is considered as consisting of steps. Fig. 2 shows frozen time frames where one step changes into the next. In these frames, only one supporting pad is shown. This supporting pad is closest to the drill periphery point P_R in axial directing and hereafter is referred to as the leading supporting pad. The second supporting pad is then referred to as the trailing supporting pad.

Frame 1 in Fig. 2 shows the initial drill position where point M touches the face of the workpiece. After the feed

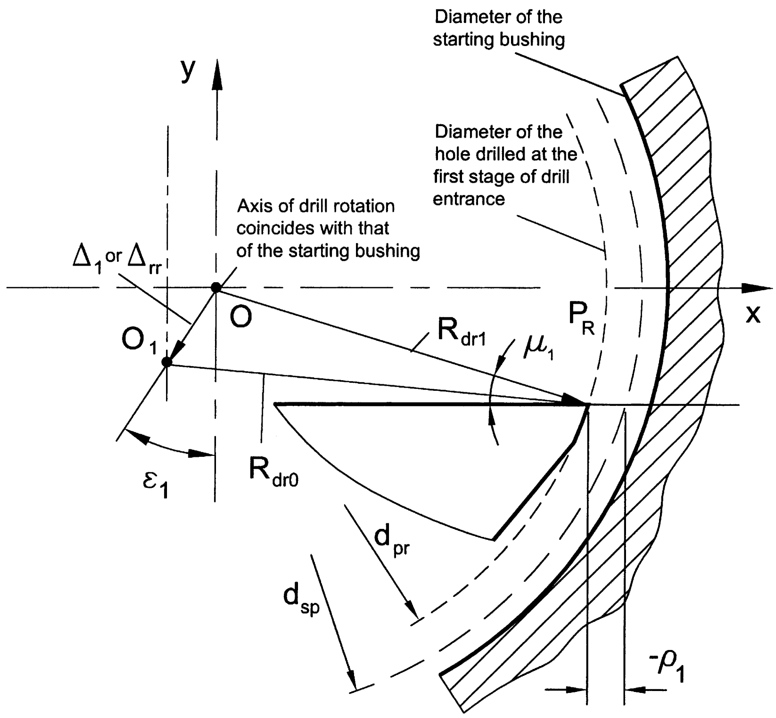

Fig. 1. Geometrical model to calculate the diameter of the hole after the first stage of drill entrance when there is no misalignment.

is applied and the first stage of drill entrance is over (discussed in Part 1), the hole of diameter d_{01} would be drilled during the considered first step.

Frame 2 in Fig. 2 shows the end of the first step of bell mouth formation when the front face of the supporting pad comes in contact with the workpiece. As seen, the length a_6 of the hole having diameter d_{01} calculates as

$$a_6 = a_1 - 0.5(d_{sb} - d_{01})\tan\varphi_f \quad (12)$$

As seen, the clearance ξ between the face of the workpiece and that of the starting bush (Fig. 3) does not play a significant role here.

The next step of bell mouth formation begins when the front face of the leading supporting pad comes into contact with the workpiece as shown in Fig. 2, Frame 2. Because the axial feed is still applied, this face deforms the edge of the hole of d_{01} diameter. As a result, the contact force F_c comes into picture. Its radial component F_{cr} forces the drill to move in the radial direction in addition to the axial feed motion. Because the drill is a rigid body, the periphery point P_R also moves in the same direction. A particular trajectory of this motion of the point P_R depends mainly on the ductility of the work material, the front angle of the supporting pad(s), φ_f, and on the shape and surface conditions of the front face of the supporting pad.

During this motion, the side cutting edge cuts the work material in order to increase the diameter from d_{01} to d_{02} and the front face of the leading supporting pad deforms the work material due to the feed motion. This deforming process leaves a character mark(s) on this front face. When such a mark appears, the common perception is that the interference of the drill flanks and the bottom of the hole being drilled took place. The common solution to the problem is thus to increase the distance a_1 and angle φ_f. Normally, in the practice of deep-hole machining, it is accomplished by grinding this face further down to increase angle φ_f. Unfortunately, this operation is often done by hand grinding where the distance a_1 and angle φ_f are out of the control of the drill designer. It should be stated here that this common *solution is inadequate* because it aims to increase a_1. The application of this solution makes the drilling conditions even worse and should never be applied because the entire load is shifted to the side cutting edge. To solve the problem, the front angle φ_f of the leading and trailing supporting pads should be reduced up to 10–15° on a short chamfer (0.08–0.12 mm) adjacent to the front apex. Besides, the clearance between the drill and the starting bush (the difference $d_{sb} - d_{dr}$) should be minimized by changing the starting bush.

Frame 3 in Fig. 2 shows the end of the discussed combined motion. As seen, the drill produces a hole of diameter d_{02}, which is equal to the drill diameter d_{dr}, and its axis coincides with the axis of drill rotation. During the time interval between Frames 2 and 3 the diameter of the hole being drilled increases from d_{01} to d_{02} and the side cutting edge plays an important role. Depending upon a particular drill design, two cases are possible in the transition from d_{02} into d_{03}:

- The first case takes place when a carbide insert is used

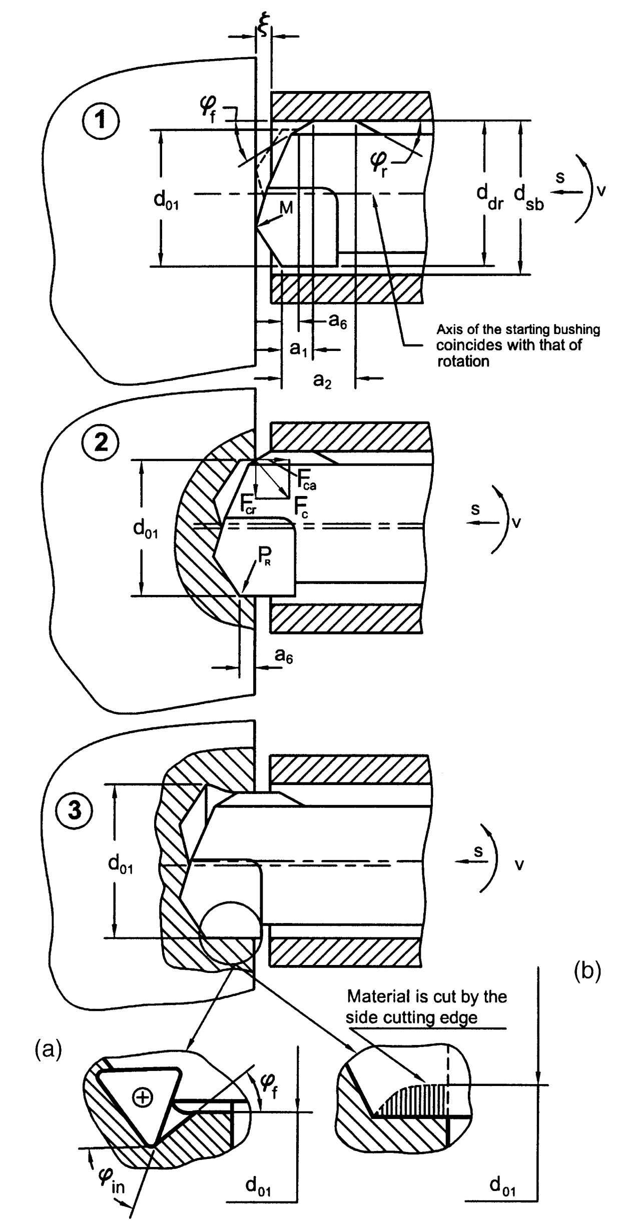

Fig. 2. Steps in bell mouth formation.

as the periphery cutting element as shown in Fig. 2—Frame 3a. As such, if the auxiliary cutting edge angle $\varphi_{in} \geq \varphi_f$ then the insert cuts the transitional conical surface starting from d_{02} at the distance a_4 and thus leaving the part of the hole having diameter d_{01} and length a_4 untouched. As a result, the front faces of the supporting pads should deform this part spreading it over the surface of the machined hole. It is understood that the severity of such deformation would depend on many parameters. Among these parameters, the following play important roles: ductility of the work material (its plastic stress–strain behavior), the clearance in the starting bush, design and location of the supporting pads.

- The second case is more common for gundrills where the side cutting edge is ground straight (except for a very small back taper which can be safely neglected in this consideration) as shown in Fig. 2—Frame 3b. As seen, the side cutting edge cuts off the entire part having diameter d_{02} and length a_4. As in the first case, the amount of the work material to be cut depends on ductility of the work material (plastic stress–strain behavior), the clearance in the starting bush, design and parameters of the supporting pads.

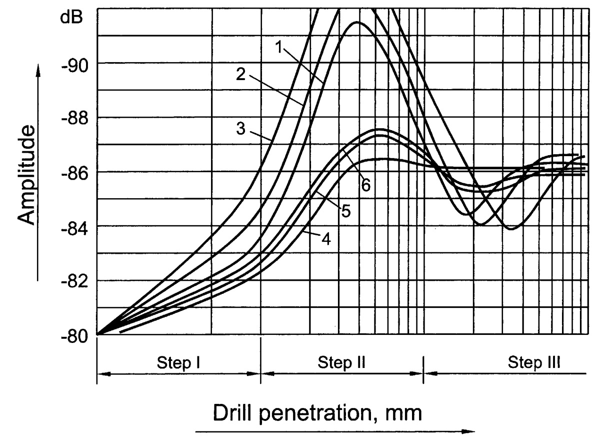

Fig. 3. Comparison of the intensity of transverse vibrations at the drill entrance for a gundrill with the supporting continuum (curve 1–3) (Star Cutter Co.) and that with two supporting pad (curves 4–6) (ASTVIK 15-03-02 design by Hyper Tool Co.). Gundrills of 8 mm dia., workpiece material—aluminum alloy 316. Curves 1,4—5800 rpm, 710 mm/min; 2,5—6800 rpm, 850 mm/min, 3,6—8000 rpm, 1060 mm/min.

Fig. 3 presents a typical example of the results of measurements of the intensity of the transverse drill vibrations at the entrance. As seen, the change from Step I to Step II, i.e. when the front face of the leading supporting pad touches the workpiece, associates with the inflection point on the amplitude diagram due to the contact force F_c. The change from Step II to Step III is also associated with the inflection point on the amplitude diagram and thus is due to the change in the direction of drill radial motion.

Fig. 4 shows that the phases of fluctuations of the axial and radial forces are opposite at the entrance. This fact is attributed to different paths traced by the cutting edges and the supporting pads. The results presented in Figs. 3 and 4 confirm the described mechanism of bell mouth formation and the conclusion of the inherent instability of gundrills with the supporting continuum.

3. Location of the supporting pads

It was already discussed in Part 1 that the location of the supporting pads of a gundrill defines its stability. It was also discussed that when a gundrill works, the cut-

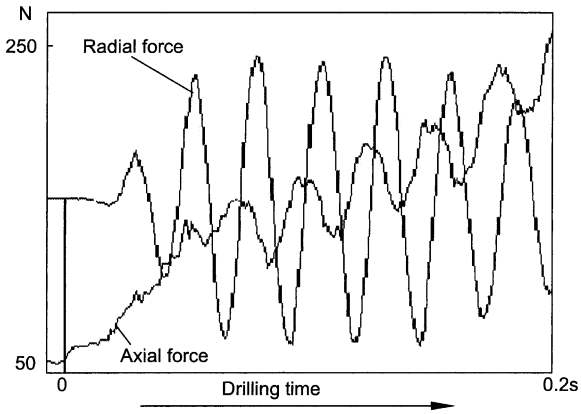

Fig. 4. Superimposed trace of axial and radial forces showing their phase relation.

ting force is generated due to the resistance of the workpiece material. This force is a 3-D vector applied at a certain point of the cutting edge. Its tangential and radial components (forces), F_T and F_R sum to create force F_{xy} (acts in the *xy*-plane) which (in contrast to other axial tools as twist drills, reamers, end milling tools) generally is not balanced, regardless of the number of the cutting edges used.

Fig. 5(a) shows the forces in the *xy*-plane due to cutting: the resultant force F_{xy}, the tangential F_T and radial F_R forces. In this figure, angles ε_1 and ξ_{xy} are location angles of F_{xy} with respect to the *y*- and *x*-axis, respectively. This figure also shows the location angles ψ_a and ψ_b of the supporting pad a and b with respect to the *x*-axis, and the central angle between these pads, ψ_{ab}.

If one compares Fig. 3 of Part 1 and Fig. 5(a), it may be noticed that in the latter the forces in the *xy*-plane are applied at the coordinate origin while in Fig. 3 of Part 1 the point of their application is located at certain distance (defined later in Part 1 as m_1) from the *y*-axis. The difference, which is simply parallel displacement of the force's origin, is taken care of by the application of a moment equal to

$$M_s = F_T m_1 \quad (13)$$

which is called the resistant moment. Its magnitude is equal to and its direction is opposite to the drilling torque.

The optimum location of the supporting pads is achieved when their normal forces F_{Na} and F_{Nb} (due to action of the resultant force F_{xy}) become equal. The analysis of the force system shown in Fig. 5(b) reveals that it is impossible to achieve equal normal forces on the supporting pads by keeping their symmetrical location relative to the action angle ξ_{xy} of the resultant force F_{xy} as follows in Fig. 6.

The problem is that the friction coefficient μ is stable and so are the friction forces F_{fa} and F_{fb} only when the supporting pads slide in the starting bush. At the entrance, μ changes over each step of drill entrance because the amount of plastic deformation done by the supporting pads changes continuously. With increase in μ, as it happens when the leading supporting pad (pad a) enters the workpiece, the normal reactions on the supporting pads change in different ways (Fig. 7). The reaction on the trailing supporting pad (pad b) increases under any relative position of the pads, but the rate of this increase is higher when the angle between the supporting pads ψ_{ab} is larger.

The normal reaction of the leading pad (pad a) depends to a large degree on the location of the trailing pad. The increase of μ may lead to a significant increase of F_{Na} (when $\psi_b \approx \xi_{xy}$) as well as to its significant decrease (when $\psi_b \ll \xi_{xy}$). It is seen in Fig. 7 that under such conditions the loss of stability can occur due separation of the leading supporting pad from the bore surface, i.e. when $(F_{N1}/F_{xy}) < 0$ even though the resultant force F_{Na} is located in the limits of the included angle ψ_{ab}, i.e. drill should be stable according to the existent stability concept [1].

Analysis of the model shown in Fig. 5(b) shows that when $\mu \neq 0$, the condition of the pads' equal load is achieved under their unsymmetrical location relative to the direction of F_{xy}. In this case, the system becomes self-stabilizing when the optimum location angles are

$$\psi_{a-opt} = \frac{\pi}{2} + \varepsilon_1 - \arccos q_{na} + \chi \quad (14)$$

$$\psi_{a-opt} = \frac{\pi}{2} + \varepsilon_1 + \arccos q_{na} + \chi \quad (15)$$

Here ε_1 is the angle between the resultant force F_{xy} and the *y*-axis, which can be calculated using the considerations presented in Section 4.2 of Part 1 as

$$\varepsilon_1 = \arctan[(R_{dr} - md)\cos^{x_k-1}\varphi_1 - md\cos^{x_k-1}\varphi_2]\frac{C_R f^{x_k}}{F_T} \quad (16)$$

q_{na} and q_{nb} are pads' parameters given by

$$q_{na} = \frac{F_{Na}}{F_{xy}}, q_{nb} = \frac{F_{Nb}}{F_{xy}} \quad (17)$$

When a gundrill is self-stabilizing, the condition of equal pads load is

$$q_{na} = q_{nb} = \frac{0.5}{u} \quad (18)$$

and parameter *u* depends upon the central angle between the pads, ψ_{ab} as shown in Fig. 8.χ is the angle of action of the resultant force R_{xy} (Fig. 5b)

$$\chi = \arcsin\left[\frac{F_{Nb}}{F_T}\mu\cos\varepsilon_1\sin\psi_{ab}\right] \quad (19)$$

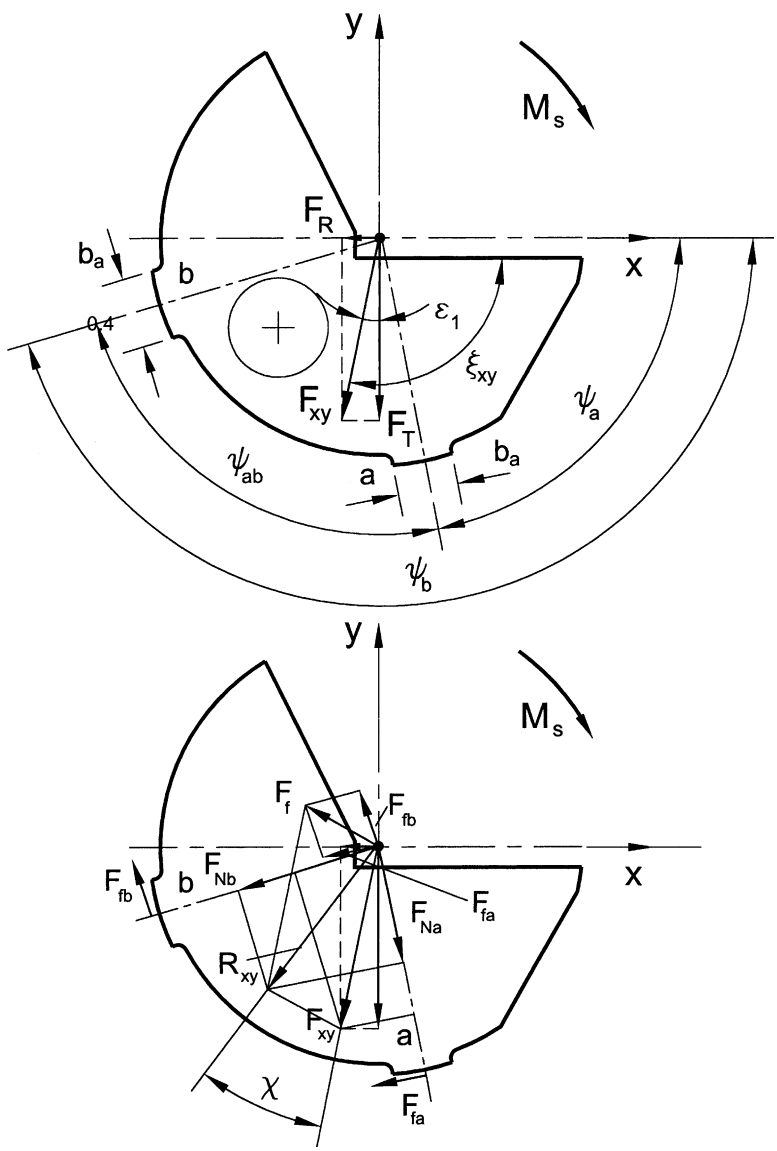

Fig. 5. Model of forces acting on the gundrill.

Fig. 9 shows the example of determination of the optimum location angles of the supporting pad under given design conditions. For comparison, the experimental points are also shown in this figure.

4. Conclusions

The following conclusions can be summarized:

1. The initial diameter of the hole being drilled depends on the clearance in the starting bush and on the tool geometry through the location angle of the resultant force in the *xy*-plane. Our analysis of Eqs. (2)–(8) and experimental data show that under the same working conditions, this diameter is always higher for gundrills with the supporting continuum compared to those with two supporting pads.
2. The distance between the drill periphery point and the front apex of the leading supporting pad is the chief factor affecting the duration of entrance instability under a given feed rate. To reduce the duration of entrance instability this distance should be kept at minimum. Although this minimum would depend on the accuracy of the whole gundrilling system, $a_1 = 0.5f$ where f the feed per revolution should be considered as the target.
3. During the drill entrance, the face of the leading supporting pad deforms the workpiece. This deforming process leaves a character mark(s) on this front face. Depending on the ductility of the work material, properties of the cutting fluid, and design parameters

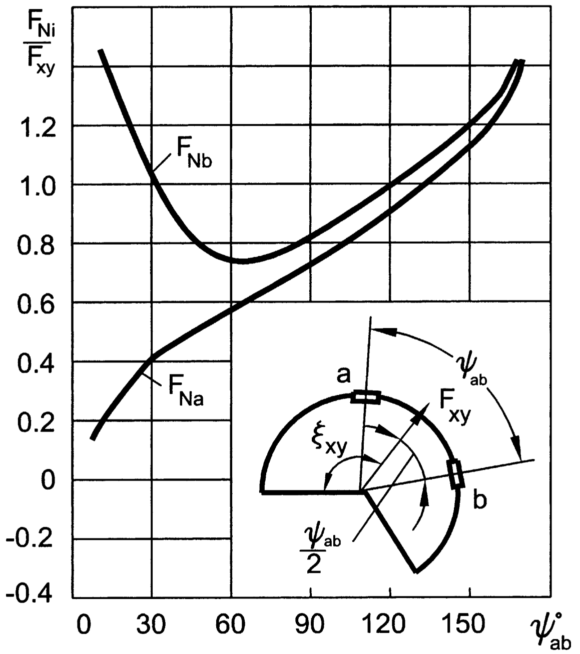

Fig. 6. The relationship $F_{Ni}/F_{xy} = f(\psi)$ under symmetrical location of the supporting pads relative to the resultant force F_{xy}.

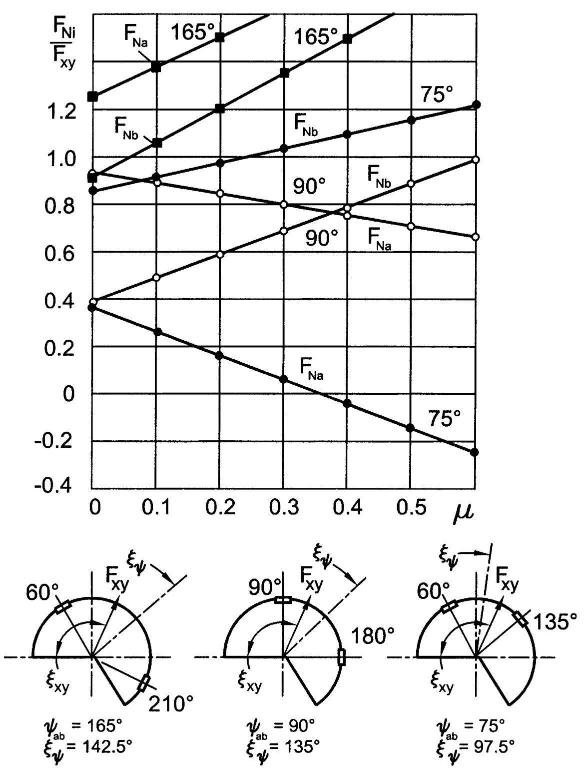

Fig. 7. The relationship $F_{Ni}/F_{xy} = f(\mu)$ for different locations of the supporting pads.

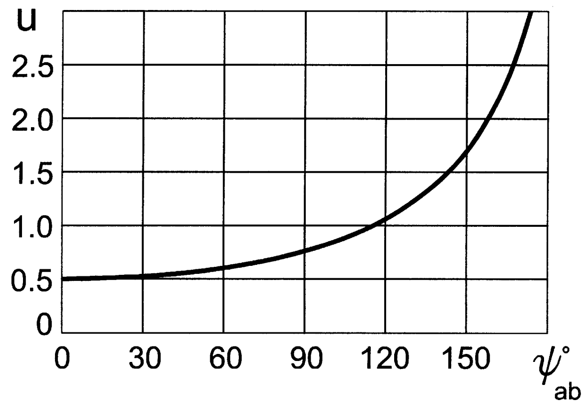

Fig. 8. The relationship $u = f(\psi_{ab})$.

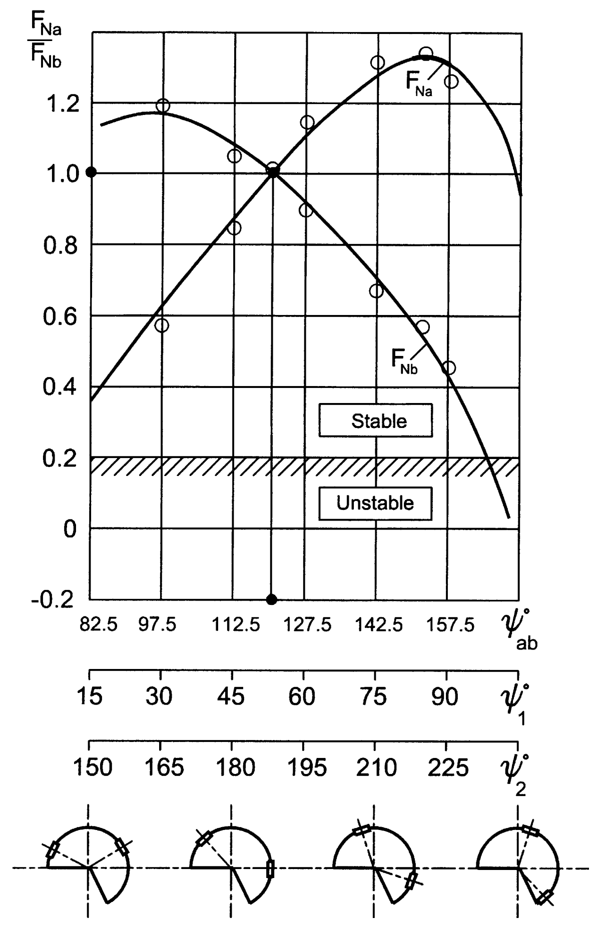

Fig. 9. Finding the optimum location angles of the supporting pads under given $\psi_{ab} = 135°$, $\mu = 0.15$. Experimental points are shown for ASTVIK 15-03-02 design by Hyper Tool Co. Gundrilling regime was: rotation speed 6800 rpm, feed rate 850 mm/min, cutting fluid flow rate 12 l/min.

of the gundrill (particularly, d_{dr} and φ_f), the appearance of this mark varies from simple screeches noticeable by an experienced professional to the built-up of the work material on the front face, which can be noticed by anyone. When such a mark appears, the common perception is that the interference of the drill flanks and the bottom of the hole being drilled took place. The common solution to the problem is thus to increase the distance a_1 and angle φ_f. Normally, in the practice of deep-hole machining, it is accomplished by grinding this face further down to increase angle φ_f. Unfortunately, this operation is often done by hand grinding where the distance a_1 and angle φ_f are out of the control of the drill designer. It should be stated here that this common solution is inadequate because the drill design has little to do with this mark. This solution makes the drilling conditions even worse and should never be applied because the entire load is shifted to the side cutting edge. To solve the problem, the front angle φ_f of the leading and trailing supporting pads should be reduced up to 10–15° on a short chamfer (0.08–0.12 mm) adjacent to the front apex. Besides, the clearance between the drill and the starting bush (the difference $d_{sb}-d_{dr}$) should be minimized by changing the starting bush.

4. During the entrance, the side cutting edge performs the actual cutting. The mechanics of this cutting is complicated because this edge rotates and due to the fact that design of this cutting edge is not meant for actual cutting. To reduce severity of additional loads on the side cutting edge the size of the circular margin ground on the flank (relief) surface of the cutting edge should be reduced when it is not possible to decrease the clearance in the starting bush.
5. The optimum location of the supporting pads is achieved when the normal forces on these pads become equal.

Acknowledgements

The support for this work by the Ford Motor Co. is gratefully acknowledged. The author also wishes to thank Mr John Gorse at Hyper Tool Co for his assistance in the experiments.

References

[1] F. Bloch, Self-Piloting Drilling, Trepanning, and Deep Hole Machining. Manufacturing Data, ASTME, Dearborn, MI, 1967.
[2] V.P. Astakhov, Gundrilling: know how, Cutting Tool Engineering 53 (12) (2001) 34–38.
[3] C.-S. Deng, J.-C. Huang, J.-H. Chin, Effect of support misalignments in deep-hole drill shafts on hole straightness, International Journal of Machine Tools and Manufacture 41 (2001) 1165–1188.
[4] V.P. Astakhov, The mechanisms of bell mouth formation in gundrilling when the drill rotates and the workpiece is stationary. Part 1: The first stage of drill entrance, International Journal of Machine Tools and Manufacture (2002).
[5] V.P. Astakhov, V.V. Galitsky, M.O.M. Osman, A novel approach to the design of self-piloting drills. Part 1. Geometry of the cutting tip and grinding process, ASME Journal of Engineering for Industry 117 (1995) 453–463.
[6] V.P. Astakhov, S.V. Shvets, A system concept in metal cutting, Journal of Material Processing Technology 79 (1998) 189–199.
[7] V.P. Astakhov, Mechanics of Metal Cutting, CRC Press, Boca Raton, 1999.